A Mean-Value Model for Control of Homogeneous Charge Compression Ignition (HCCI) Engines

D. J. Rausen

A. G. Stefanopoulou[1]
e-mail: annastef@umich.edu

The University of Michigan, Ann Arbor, Michigan 48109, USA

J.-M. Kang

J. A. Eng

T.-W. Kuo

General Motors Corporation, Warren, Michigan 48090, USA

A Mean Value Model (MVM) for a Homogeneous Charge Compression Ignition (HCCI) engine is presented. Using a phenomenological zero-dimensional approach with five continuous and three discrete states we first model the effects of the Exhaust Gas Recirculation (EGR) valve, the exhaust Rebreathing Lift (RBL), and the fueling rate on the state of charge in the cylinder at intake valve closing. An Arrhenius integral is then used to model the start of combustion, θ_{soc}. A series of simple algebraic relations that captures the combustion duration and heat release is finally used to model the state of charge after the HCCI combustion and the Location of Peak Pressure (LPP). The model is parametrized and validated using steady-state test data from an experimental gasoline engine at the General Motors Corporation. The simple model captures the temperature, pressure, air-to-fuel ratio, and inert gas fraction of the exhausted mass flow. This characterization is important for the overall HCCI dynamics because the thermodynamic state (pressure, temperature) and concentration (oxygen and inert gas) of the exhausted mass flow affect the next combustion event. The high dilution level in HCCI engines increases the significance of this internal feedback that generally exists to a smaller extent in conventional spark-ignition and compression-ignition internal combustion engines.
[DOI: 10.1115/1.1985439]

1 Introduction

The basis of Homogeneous Charge Compression Ignition (HCCI) engines is their fast and flameless combustion after an autoignition process of a homegeneous mixture. HCCI combustion achieves high fuel efficiency [1] with low NOx emissions due to the limited cylinder peak temperature (below 1700 K). The timing of HCCI combustion is determined by mixture conditions, rather than the spark timing or the fuel injection timing that are used to initiate combustion in Otto and Diesel engines, respectively. Instead, controlled autoignition requires regulation of the mixture properties (temperature, pressure, and composition) at the Intake Valve Closing (IVC). Observations show that Variable Valve Timing (VVT) flexibility can provide control over the mixture conditions at IVC [2,3]. For example, early Exhaust Valve Closing (eEVC) and late Intake Valve Opening (*l*IVO) enable internal EGR (iEGR) with high temperature trapped residuals, which also alleviates the preheating need [4]. To control hot residuals (internal Exhaust Gas Recirculation or iEGR), we consider in this paper an actuation technique called exhaust rebreathing, in which the exhaust valve is reopened during the intake stroke, as shown in Fig. 1. A conventional EGR valve allows control of the external Exhaust Gas Recirculation (eEGR) and thus the cold fraction of the inert mass trapped at IVC.

Control synthesis and design requires a model that represents the effects of the valve actuators to the charge conditions and the HCCI combustion characteristics. Phenomenological crank angle-resolved HCCI combustion models have been developed originally in [1] and recently in [5]. Although these models are indispensable for understanding and simulating HCCI combustion, low-order models are necessary for real-time feedback and observer design. Efforts to extract information from the crank angle-resolved models and control the peak cylinder pressure of propane-based HCCI combustion are presented in [6]. A simple simulation model of HCCI engine was used for control in [7]. Input-output models based on system identification are shown in [8] and used for control of the combustion timing with dual fuel. Papers that present experimental results with controlled HCCI combustion through in-cylinder pressure or ion current feedback have used decoupled (single-input single-output) control laws. In [9] three decentralized PI controllers for an inlet heater, fuel charge, and fuel octane ratio are used to regulate inlet temperature to 80 deg, track IMEP commands, and regulate 50 percent burn timing (CA50) to a range of 3°–8° ATDC. The last control goal is the hardest to achieve. In two recent papers [10,11], PI controllers are used for intake valve closing or negative overlap. The authors anticipate better results with model-based tuning of the controller gains and coordination of all the available actuators.

To this end we develop in [12] a Mean Value Model (MVM) that captures the effects of the exhaust valve rebreathing lift u_{rbl}, the EGR valve u_{egr}, and the gasoline fueling rate W_f to the charge composition and combustion characteristics. Specifically, we consider as performance variables the air-to-fuel ratio (AFR) at the exhaust tailpipe and the crank angle of 50% fuel burned, θ_{CA50}. We assume the availability of a wide range, fast, heated Exhaust Gas Oxygen (EGO) sensor for AFR measurements in the exhaust manifold AFR_{EGO}. In summary, we develop the appropriate model for regulating AFR and θ_{CA50} by coordinating the rebreathing valve lift u_{rbl}, and the EGR valve u_{egr} during step changes in fueling rate W_f and constant engine speed N. The input-output signals are shown in Fig. 2. Note here that we consider engine speed as a system parameter than can be potentially treated as another exogenous signal. Engine speed, due to its effects on EGR amount and available duration for combustion [4], should also be taken into account in the HCCI model. Published experimental results [10,9] show large deviations of combustion timing during

[1]Corresponding author. E-mail: annastef@umich.edu, Phone:+1(734)615-8461
Contributed by the Dynamic Systems, Measurement, and Control Division of THE AMERICAN SOCIETY OF MECHANICAL ENGINEERS for publication in the ASME JOURNAL OF DYNAMIC SYSTEMS, MEASUREMENT, AND CONTROL. Manuscript received: October 26, 2003. Final revision: August 23, 2004. Associate Editor: Matt Franchek.

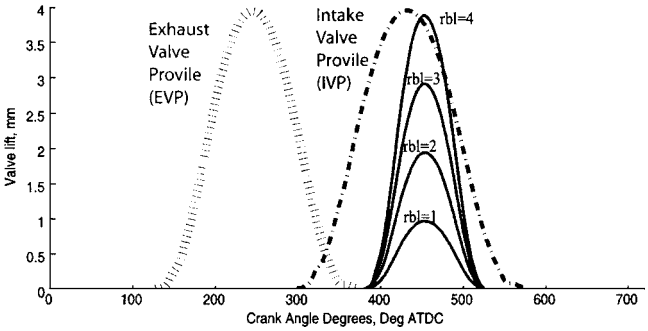

Fig. 1 Exhaust, intake, and rebreathing valve profiles

changes in speed, even during closed loop control. Thus, we anticipate substantial challenges associated with speed changes in the future.

2 Model Structure

The model presented here includes a physics-based parameterization of HCCI behavior. The MVM dynamical behavior is associated with (i) states representing the mass composition and pressures in the intake and exhaust manifold volumes and (ii) the delay between cylinder intake and exhaust processes. The cylinder is modeled as a pump (see Fig. 3 as compared to Fig. 2) based on (a) cycle-average cylinder flows and (b) temperature out of the cylinder (cycle-sampled exhaust runner temperature) T_{er}. The main parameters of the MVM are depicted in the schematic diagram of Fig. 3. The intake manifold is referred to as volume 1, the exhaust manifold volume as volume 2, and the cylinder as volume c. Variables associated with ambient conditions are denoted with subscript 0. States or variables associated with masses at volume x are called m_x and those associated with pressures are called p_x. To account for composition dynamics, burned gas fraction b_x at volume x is defined as

$$b_x = \frac{\text{mass of burned gas in } x}{\text{total mass in } x} = \frac{m_x^b}{m_x} \tag{1}$$

where m_x^b is the mass of burned gas (combustion products including excess oxygen) at volume x. Since the HCCI engine operates lean, both the flow through the EGR valve and the rebreathed residuals contain air. Mixture compositions therefore include three components: air, fuel, and burned gas.

A description of the model's eight dynamic equations, represented by five state equations and three delays, is presented in Sec. 4. The five model states defined by differential equations are shown in rectangular boxes in Fig. 3. Flows are depicted according to the notation W_{xy}, where x is the source of the flow and y is the sink. The exhaust flow, W_{c2}, from cylinder to exhaust is considered as a delayed sum of the flows into the cylinder, as described later in Eq. (4). The other two delayed states correspond to the exhaust runner gas temperature, T_{er}, and burned gas fraction, b_{er}.

The MVM is parametrized using steady-state test data collected from a single-cylinder engine described in Sec. 3. The combustion process is considered as a series of causal algebraic relations whereby conditions at Intake Valve Closing (IVC) determine those at Exhaust Valve Opening (EVO). The combustion model provides the composition and temperature of the gas that is exhausted and fed back to the cylinder through eEGR and iEGR, representing internal feedback from the Manifold Filling Dynamics (MFD) through the HCCI combustion and back to the MFD. The integrated model, shown in Fig. 4 captures both the steady-state and dynamical relations between the inputs and outputs. The model is accurate for dynamics slower than the cycle period, or those below $\omega_v = 2N\pi/120$ rad/sec, where N is in rev/min.

3 Experimental Setup

Dynamometer experiments used to parametrize the MVM were performed on a single-cylinder, gasoline, engine (86 mm bore, 94.6 mm stroke, 0.55 L displacement, compression ratio CR=14) at 1000 RPM and a range of fueling levels. The cylinder head includes four valves, a pent-roof combustion chamber, and a spark plug that was not activated during these experiments.

Sonic nozzles measured airflow, and two large plenums damped intake pressure pulsations. Plenums heaters maintained intake air temperature of 90°C. Even with internal exhaust gas recirculation, there is a severe limitation on the lowest fueling levels that the engine can be operated at. Intake air heating to 90°C helps to operate the engine at lower fueling rates. This charge heating can easily be obtained by using a water-to-air heat exchanger in the intake (similar to turbocharged engines). This exchanger also buffers the engine from ambient temperature changes. External heat exchangers maintained air and water temperatures at 95°C. Fuel flow was measured with a Pierburg PLU 103B flow meter. Exhaust gas recirculation (EGR), controlled manually via a ball valve, was mixed with the fresh air and fuel mixture upstream of the engine in the first intake plenum. The amount of external EGR is determined from the emissions measurements and CO_2 levels in the intake. It can be set to any desired level at steady-state conditions. The emissions data is sampled for 2 min at each operating condition.

A Kistler 6125 pressure transducer located at the rear of the combustion chamber along the axis of the pent roof was amplified with a Kistler 504E charge amplifier. The Crankshaft position was measured with a Dynapar crankshaft encoder, and a hall-effect sensor provided camshaft location. A Sensotec strain gage transducer provided intake manifold pressure, which calibrated the cylinder pressure reading at the bottom of the intake stroke. Cylinder

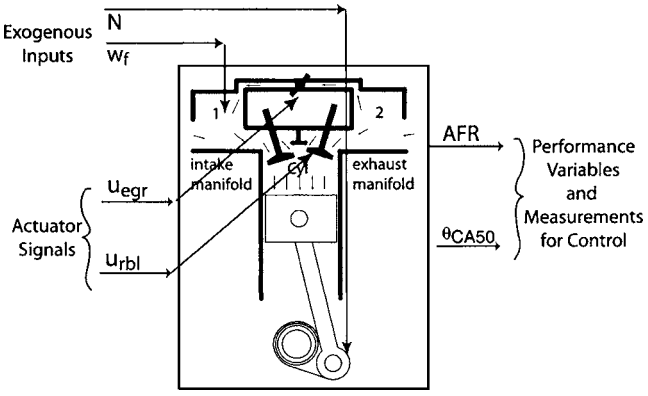

Fig. 2 Definition of input-output HCCI engine signals

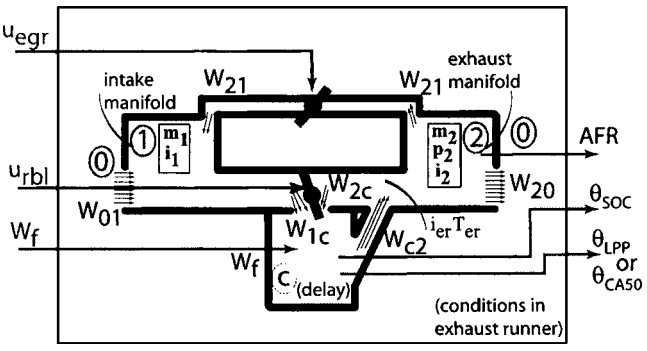

Fig. 3 Schematic diagram and notation for the mean value model

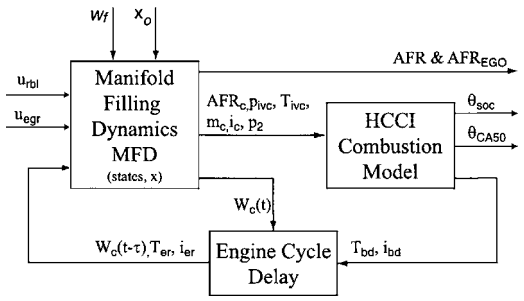

Fig. 4 The integrated mean value model, consisting of Manifold Filling Dynamics (MFD) and HCCI combustion model

pressure data was recorded using the MTS-DSP Advanced Combustion Analysis Program (ACAP) that calculates performance parameters such as Peak Pressure and location of peak pressure in real time. For all the experimental data collected the engine is operated at steady state. At each operating condition data from 300 engine cycles is used to obtain an ensemble-averaged pressure trace.

Since the engine is operated with exhaust rebreathing, the amount of residual gas within the cylinder has to be estimated to provide the steady-state data for the total mass and the residual trapped in the cylinder. A simple filling model using partial pressure of the intake mass and the exhaust gas temperature in the exhaust runners estimated the residual mass within the cylinder. Temperatures throughout the cycle are calculated using the ideal gas law and the estimated trapped mass, as shown in the Appendix. Standard heat release analysis was used to determine the crank angle for 1%, 50%, and 90% fuel burned that is used for the MVM parametrization and validation. The standard heat release uses the measured cylinder pressure data along with a heat transfer model (based on Sec. 12.4 of [13]) was calibrated within GM for the specific experimental engine. Cylinder blow-by was maintained in a minimal level, and thus not included in the heat release analysis. The heat of vaporization was also neglected from the heat release calculations because it is incredibly small (order of 5 J) when compared to the total energy release (order of 4000 to 450 J).

4 Manifold Filling Dynamics (MFD)

Based on the assumption of an isothermal intake manifold with $T_1=90°C$ (363 K), two states are sufficient to characterize the intake manifold: the total intake manifold mass, m_1, and burned gas fraction, b_1:

$$\frac{d}{dt}m_1 = W_{01} + W_{21} - W_{1c}$$

$$\frac{d}{dt}b_1 = \frac{-W_{01}b_1 + W_{21}(b_2 - b_1)}{m_1}. \tag{2}$$

The ideal gas law relates the intake manifold pressure p_1 to the mass by $p_1=m_1(RT_1/V_1)$ where V_1 is the intake manifold volume. The thermodynamic constants are the difference of specific heats at constant pressure and constant volume [R, kJ/(kg K)] and the ratio of these specific heats (γ). The dependence of these variables on the gas composition has been neglected. Note that we also neglect the transport delays in the pipes for the EGR. We assume here that ($p_1<p_0<p_2$) so that all the flows through the valves and orifices are due to the pressure difference between the volumes and the flow from the intake manifold to the cylinder W_{1c} is a forced flow due to cylinder pumping.

$$\frac{d}{dt}m_2 = W_{c2} - W_{20} - W_{21} - W_{2c}$$

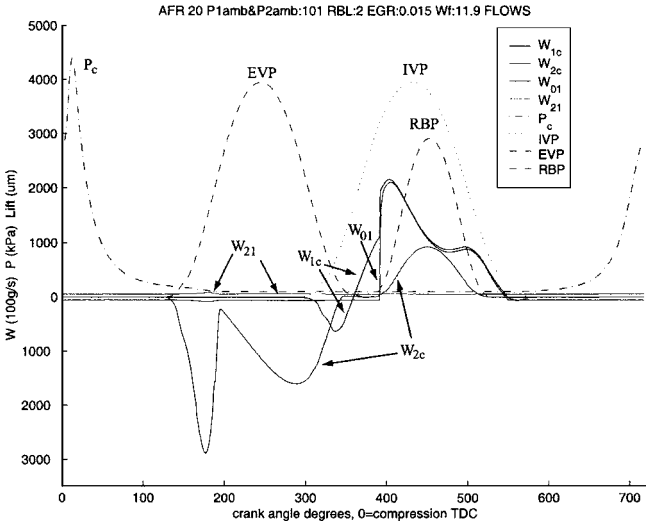

Fig. 5 Cylinder flow and other crank angle-resolved variables

$$\frac{d}{dt}b_2 = \frac{W_{c2}(b_{er} - b_2)}{m_2} \tag{3}$$

$$\frac{d}{dt}p_2 = \frac{\gamma R}{V_2}(W_{c2}\tilde{T}_{er} - (W_{20} + W_{21} + W_{2c})T_2),$$

Three states represent the gas filling dynamics in the exhaust manifold: mass, m_2, pressure, p_2, and burned gas fraction, b_2. V_2 is the volume of the exhaust manifold. The temperature of the gas entering the exhaust manifold is $\tilde{T}_{er}=T_{er}-\Delta T_{er2}$ where ΔT_{er2} is a temperature drop of 75°C, based on test data, from the exhaust runner temperature (T_{er}). The ideal gas law relates the temperature to the pressure and mass values: $T_2=p_2V_2/(Rm_2)$. W_{c2} is the average mass flow rate from the cylinder to the exhaust manifold, calculated as delayed cycle-sampled total flow into the cylinder:

$$W_{c2}(t+\tau) = W_{1c}(t) + W_f(t) + W_{2c}(t). \tag{4}$$

The temperature, T_{er}, and burned gas fraction, b_{er}, of the mass flow through the exhaust runner are also calculated via delays:

$$T_{er}(t+\tau) = T_{bd}(t) \tag{5}$$

$$b_{er}(t+\tau) = b_{bd}(t) \tag{6}$$

where T_{bd} and b_{bd} are the temperature and burned gas fraction, respectively, of the blowdown gas into the exhaust runner. These quantities are calculated in the last phase of the combustion model, presented in Sec. 7.3. The engine cycle duration $\tau=N/120$, where N is the engine speed (rev/min), represents the cycle delay imposed by the engine's cyclic behavior. Note here that the differential equations (2) and (3) can be discretized using the Euler's method on an interval equal to the engine cycle. For higher fidelity we leave the manifold filing dynamics of Eqs. (2) and (3) in the continuous-in-time domain and interface with the discrete-in-time cylinder delay dynamics of Eqs. (4)–(6) with a sample and zeroth-order hold (ZOH).

The flows W_{xy} from volume x to volume y are based on an orifice flow equation (Appendix C of [13]). The EGR flow W_{21}, via the EGR valve effective flow area $C_dA_{egr}(u_{egr})$ is determined by u_{egr}.

5 Cycle-Average Cylinder Flow

The mean flows into the cylinder, W_{1c} and W_{2c}, are calculated

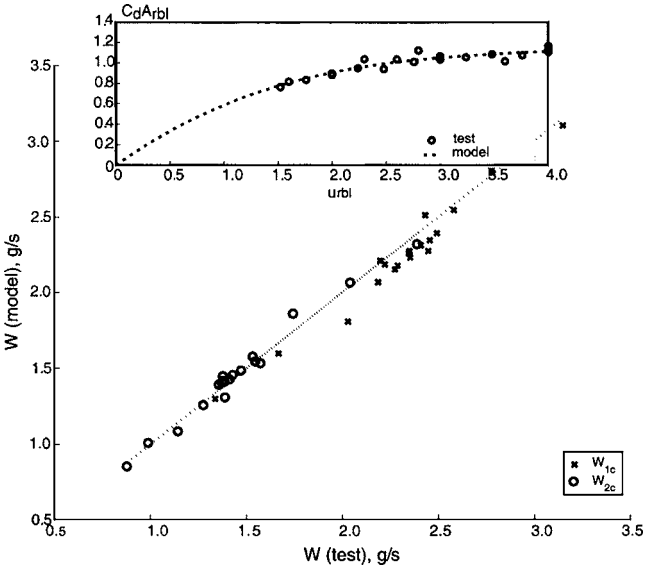

Fig. 6 Validation of predicted mean cylinder flows

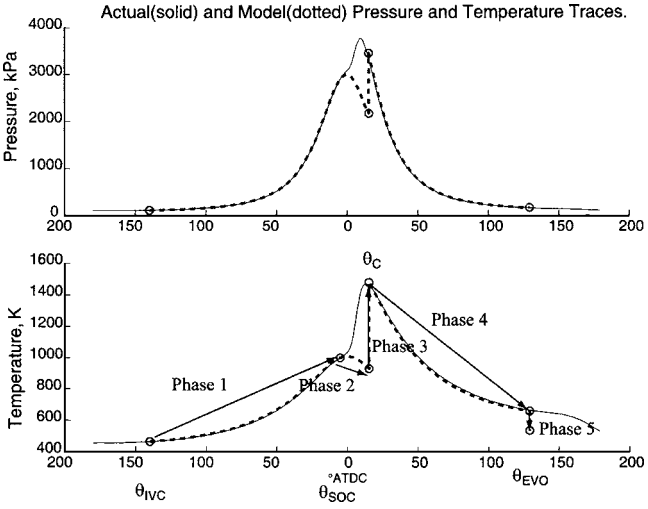

Fig. 7 Actual (solid) and estimated (dotted) pressure and temperature traces in cylinder, from before IVC to after EVO. Calculated model values are indicated with circles

$$W_{1c} = \frac{(1-x_r)}{\tau} m_c - W_f$$
$$W_{2c} = \frac{x_r}{\tau} m_c \tag{7}$$

where m_c is the trapped cylinder mass at IVC (derived in the next section), W_f is the mean fuel flow rate into all of the cylinders, and x_r is the mass fraction of internal (higher temperature) residual gases at θ_{ivc} ([13], p. 102). For the system's fixed intake valve closing angle, θ_{ivc}, and constant intake manifold temperature, T_1, x_r is parametrized by:

$$x_r = \alpha_1 \left(1 + \kappa_0 \frac{p_1^{\kappa_1}}{p_2^{\kappa_2}\sqrt{T_{\text{er}}}} \right) \frac{(u_{\text{rbl}} + \alpha_2 u_{\text{rbl}}^2 + \alpha_3 u_{\text{rbl}}^3)}{c_d A_{\text{rbl}}} \tag{8}$$

where all the α and κ coefficients have been identified using experimental data and simulations of a GM proprietary engine model with crank angle-resolved flows as shown in the specific example of Fig. 5 for u_{rbl}=3 mm.

A comparison of regressed and experimental cycle-averaged test values for the estimated flows is shown in Fig. 6. Increasing rebreathing lift correlates with a larger value of x_r, but the sensitivity of x_r to u_{rbl} decreases as the rebreathing lift actuator approaches its maximum value of 4 mm as shown also in Fig. 6. Rebreathing lift effectively throttles the flow through the "pump"-like cylinder.

Residual gas fraction, x_r, in the cylinder at IVC, as defined in the preceding paragraphs, is distinct from the burned gas fraction in the cylinder, b_c, which is calculated below, in (11). Residual gas fraction, x_r, defines the effect of the mean value model states, x, and the rebreathing lift, u_{rbl}, on the relative magnitudes of the mass flows, W_{1c} and W_{2c}, into the cylinder. Burned gas fraction in the cylinder, b_c, tracks the aggregate percentage of burned gases from these two sources.

6 Conditions at Intake Valve Closing (IVC)

We approximate cylinder pressure at IVC as a linear function of p_1:

$$p_{\text{ivc}} = \beta_0 + \beta_1 p_1. \tag{9}$$

The charge temperature at IVC is calculated as the mass-weighted average of the temperatures of the flows contributing to the trapped mass m_c:

$$T_{\text{ivc}} = T_1(1-x_r) + T_{\text{er}} x_r$$
$$m_c = \frac{p_{\text{ivc}} V_{\text{ivc}}}{R T_{\text{ivc}}}. \tag{10}$$

Note that R is fixed and tuned (within the physical range) to capture all conditions for which we had data. We do not assign different specific heats to the individual species separately because that would increase the system states.

Remaining conditions at intake valve closing that will be required by the combustion model are:

$$b_c = (1-x_r)\frac{W_{1c}}{W_{1c}+W_f} b_1 + x_r b_{\text{er}} \tag{11}$$

$$\text{AFR}_c = \frac{(1-b_1)W_{1c} + (1-b_{\text{er}})W_{2c}}{W_f} \tag{12}$$

7 HCCI Combustion Model

Assuming complete and lean combustion, b_{bd} (13) is unaffected by the combustion process and depends only on two of the conditions at IVC: b_c and AFR_c.

$$b_{\text{bd}} = \frac{\text{AFR}_s + 1}{\text{AFR}_c + 1}(1-b_c) + b_c \tag{13}$$

where AFR_s is the stoichiometric air-to-fuel ratio.

The air-to-fuel ratio from an exhaust gas oxygen sensor, AFR_{EGO}, is:

$$\frac{d}{dt}\text{AFR}_{\text{EGO}} = \frac{1}{\tau_{\text{EGO}}}(\text{AFR}_2 - \text{AFR}_{\text{EGO}})$$
$$\text{AFR}_2 = \frac{1-b_2+\text{AFR}_s}{b_2}. \tag{14}$$

EGO sensor time constant is τ_{EGO}. This expression is equivalent to an algebraic rearrangement of the expression for F_e (b_2 here) as a function of r_e (AFR_2 here) in [14].

A simplified combustion model provides the remaining variables, exhaust blowdown temperature, T_{bd}, and the performance variable, θ_{CA50} as a function of T_{ivc} and p_{ivc}. The model consists of five-sequential phases: (i) polytropic compression that leads to the start of combustion (SOC) through autoignition at θ_{soc}, (ii) a combustion duration that determines an effective θ_{CA50}, preceding

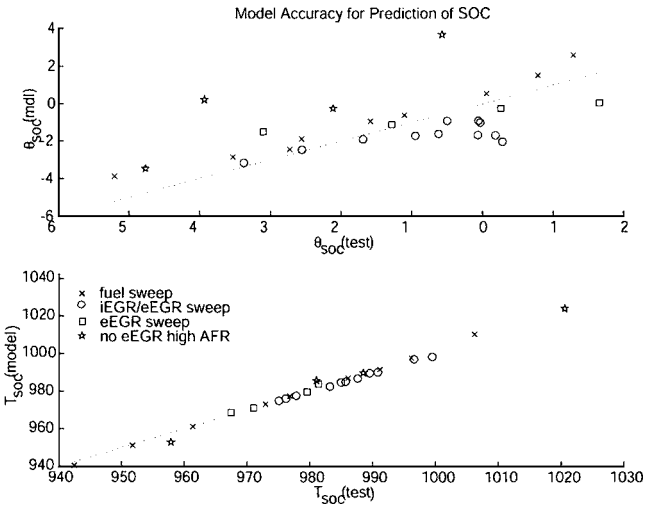

Fig. 8 Plots showing the prediction accuracy for θ_{soc} in crank-angle degrees after the top dead center and T_{soc} in K.

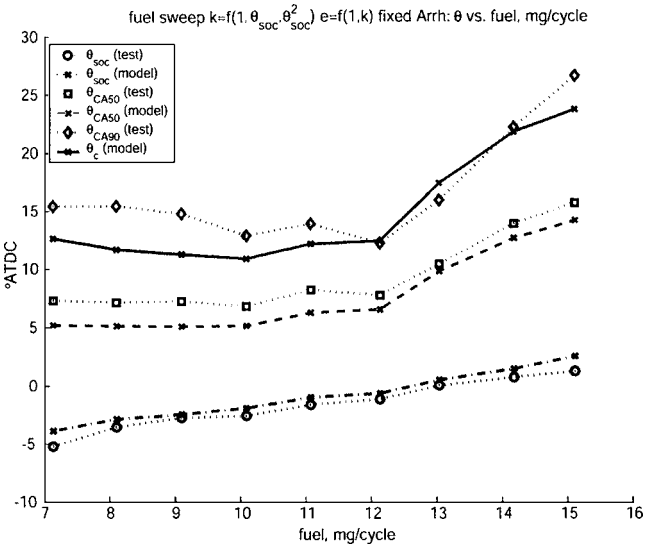

Fig. 10 A comparison of integrated combustion model predictions of θ_{soc} and resulting predictions of θ_{CA50} with test data for fuel sweep

(iii) simulated instantaneous heat release, (iv) polytropic expansion, and (v) adiabatic blowdown that yields T_{bd}. These phases are depicted in Fig. 7, where the actual (solid line) and modeled (dotted line) pressure and temperature trajectories are shown. Although cylinder pressure is measured, the cylinder temperature that we use to validate our model is not measured but determined using the measured cylinder pressure and calculations shown in the Appendix.

7.1 Phase 1: Intake Valve Closing to Start of Combustion. Motivated by [15,10,16], the Arrhenius integral is simplified and used to predict the SOC timing, θ_{SOC}:

$$\mathrm{AR}(\theta_{soc}) = 1 \text{ where } \mathrm{AR}(\theta) = \int_{\theta_{ivc}}^{\theta} RR(\vartheta)d\vartheta \tag{15}$$

and

$$\mathrm{RR}(\vartheta) = Ap_c^n(\vartheta)\exp\left(-\frac{E_a}{RT_c(\vartheta)}\right) \tag{16}$$

where T_c and p_c are cylinder temperature and pressure, respectively, during compression, A is a scaling constant, E_a is the activation energy for the autoignition reaction, and n indicates the reaction's sensitivity to pressure. We define $v_{ivc}(\vartheta) = V_c(\vartheta_{ivc})/V_c(\vartheta)$, with $V_c(\vartheta)$ the cylinder volume at crank angle ϑ, and assume polytropic compression from IVC to SOC with coefficient n_c. The Arrhenius integrand is thus simplified

$$\mathrm{RR}(\vartheta) = Ap_{ivc}^n v_{ivc}^{n_c n}(\vartheta)\exp\left(-\frac{E_a v_{ivc}^{1-n_c}(\vartheta)}{RT_{ivc}}\right) \tag{17}$$

and the coefficients A, E_a and n are selected using the crank angle of 1% fuel burned as the start of combustion $\theta_{soc}=\theta_{CA01}$. A standard nonlinear optimization routine (constr.m from MATLAB) was used to find one set of values that can capture reasonably well the crank angle of 1% fuel burned for all the experiments (fueling

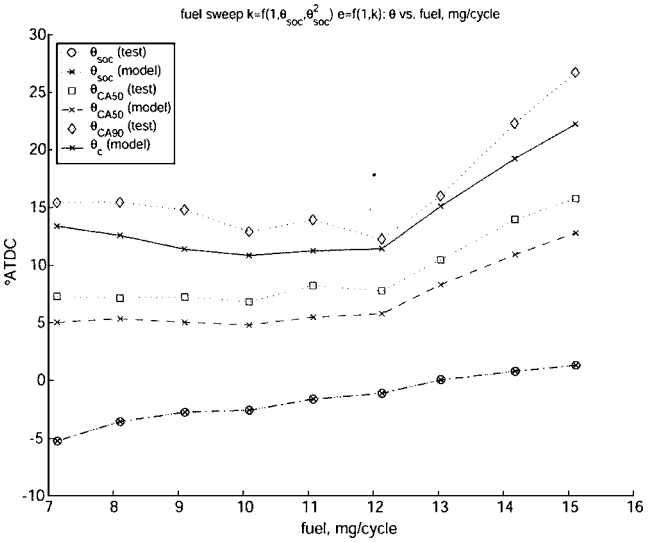

Fig. 9 Plot showing the impact of the parametrized values for k, E_c, and e on the burn duration for the fuel sweep data. To evaluate the prediction of the combustion model in Eqs. (18)–(20), we assume a perfect prediction of the SOC timing.

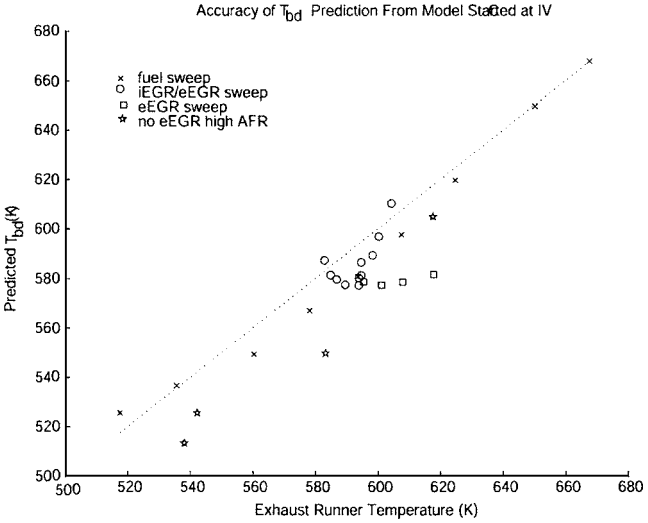

Fig. 11 Exhaust runner blowdown temperature prediction based on all five phases of the model from conditions at intake valve closing

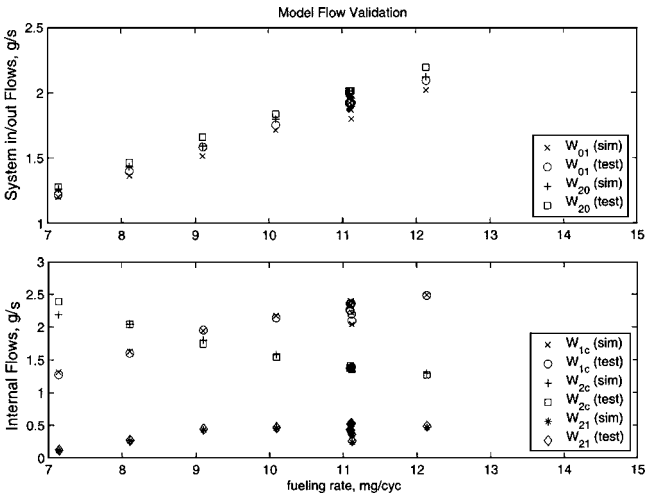

Fig. 12 Actual and simulated flows for the integrated combustion model using ambient pressure of 101 KPa connected to both intake and exhaust manifolds

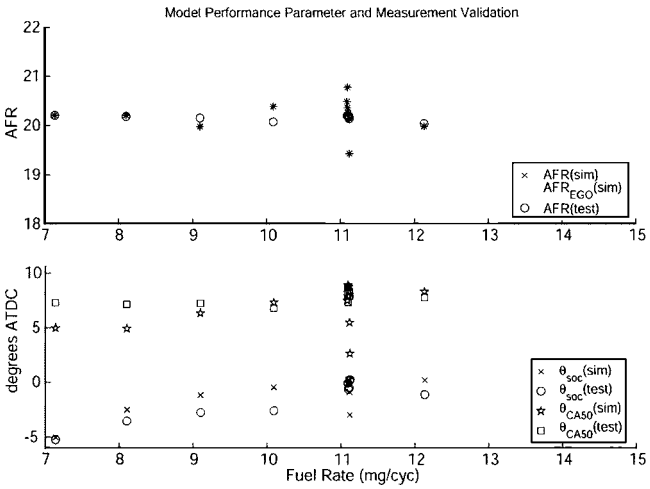

Fig. 14 Actual and simulated performance parameters and related measurements.

sweep and internal EGR rate sweep). Detailed physics-based models for the ignition timing can also be found in [15]. With θ_{soc} defined by (15)–(17), the charge temperature at SOC is $T_{soc}=T_{ivc}v_{ivc}^{(n_c-1)}(\theta_{soc})$. The resulting predictions of θ_{soc} and T_{soc} are shown in Fig. 8. The largest error is observed at conditions with high AFR (AFR$>$26) limiting the validity range of our model. This error, however, can be avoided if a good AFR controller is designed in the future.

7.2 Phase 2: Combustion Duration. We define the HCCI combustion duration $\Delta\theta$ as the crank angle degrees between 1% and 90% fuel burned. Heat release due to combustion is considered to occur instantaneously at θ_c [17,18]:

$$\theta_c = \theta_{soc} + \Delta\theta$$

$$\text{where } \Delta\theta = k(T_{soc})^{(-2/3)}(T_m)^{1/3}\exp\left(\frac{E_c}{3R_uT_m}\right)$$

$$\text{and } T_m = T_{soc} + e(1-b_c)\Delta T$$

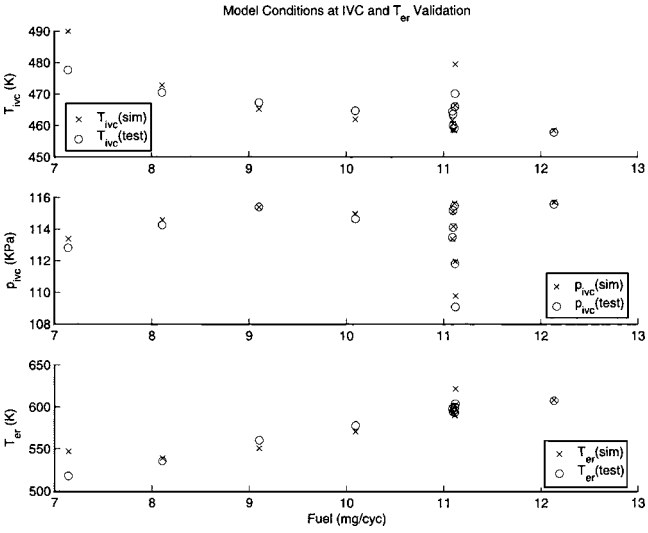

Fig. 13 Actual and simulated conditions at IVC, T_{ivc} and p_{ivc} and exhaust runner temperature, T_{er}.

$$\text{finally } \Delta T = \frac{Q_{LHV}}{c_v(1+AFR_c)}. \tag{18}$$

The parameter E_c is the activation energy of the global reaction representing the combustion process and is assumed to be 185 kJ/mol. The parameter e represents an averaging of the released thermal energy during combustion. The parameter k relates to the effective combustion duration, $\Delta\theta$, during which no heat release is modeled. As the duration lengthens, a smaller proportion, e, of the released heat contributes to an effective mean temperature, T_m during the combustion. After the combustion duration, instantaneous heat release occurs at the combustion location, θ_c. Both of the parameters k and e have been optimized to match the actual burn duration from 1% to 90%. The crank angle of 50% burned fuel is calculated as $\theta_{CA50}=\theta_{soc}+0.55\Delta\theta$.

Since e is a measure of the average temperature during combustion, a lower value of k corresponds to a shorter combustion, which also corresponds to a higher value for e. The combinations of independently optimized values of k and e results in a single relation (19) for which the value for e is uniquely determined by the value for k

$$e = a_0 + a_1k. \tag{19}$$

This yields a physically based combustion duration model whose variations over the operating range can now be captured with a single parameter, k. Optimized values of k that precisely reproduce the combustion duration for each set of test data are then parametrized as a function of θ_{soc}:

$$k = b_{k0} + b_{k1}\theta_{soc} + b_{k2}\theta_{soc}^2. \tag{20}$$

Note here that the heat transfer is captured in our model with the parameter e in Eqs. (19) and (20). The parameter e is tuned to capture the apparent fuel efficiency that lumps (i) combustion efficiency and (ii) heat losses through the walls. The accuracy of these predictions can also be seen in Fig. 9.

7.3 Phase 3: Instantaneous Heat Release. The charge temperature just before the combustion can be calculated by $T_{bc}=T_{ivc}v_{ivc}^{(n_c-1)}(\theta_c)$ and the corresponding pressure as $p_{bc}=p_{ivc}v_{ivc}^{n_c}(\theta_c)$. Assuming an instantaneous release of all of the fuel's heat, the charge temperature and pressure after the combustion are given by:

$$T_{ac} = T_{bc} + (1-b_c)\Delta T \text{ and } p_{ac} = p_{bc}T_{ac}/T_{bc} \tag{21}$$

7.4 Phase 4: Polytropic Expansion. To account for the polytropic expansion with coefficient n_e, a volume ratio analogous to $v_{\text{ivc}}(\vartheta)$ is defined as $v_c(\vartheta)=V_c(\vartheta_c)/V_c(\vartheta)$ so that the charge temperature and pressure at EVO is

$$T_{\text{evo}} = T_{ac} v_c^{(n_e-1)}(\theta_{\text{evo}}) \text{ and } p_{\text{evo}} = p_{ac} v_c^{n_e}(\theta_{\text{evo}}). \tag{22}$$

7.5 Phase 5: Exhaust Blowdown. After EVO, the exhaust temperature leaving the cylinder can be considered as

$$T_{\text{bd}} = T_{\text{evo}} \frac{p_2}{p_{\text{evo}}}^{(n_e-1)/n_e} + \Delta T_{\text{bd}} \tag{23}$$

due to the adiabatic expansion of the gas down to the exhaust manifold pressure p_2 with an offset of a constant temperature difference, ΔT_{bd}.

The model provides a minimal mathematical representation of the physical combustion process as well as a basis function based for which the six parameters, A, E_a, and n from (17) and k, E_c, and e from (21) can be tuned to fit all available data in the future. The θ_{soc} and θ_{CA50} predictions are shown in Fig. 10. The T_{bd} predictions of the HCCI Combustion model are shown in Fig. 11.

8 Validation

The HCCI engine model combines the manifold filling dynamics of Sec. 4 with the simplified combustion model presented in Sec. 7, as shown in Fig. 4. All the model values are shown in Table 1. The model runs with CPU time 0.08 s/cycle that is faster than real time at the modeled engine speed (1000 rpm). A Dell Latitude computer with Pentium III Mobile, CPU 1200 MHz, At/AT compatible with 523,644 KB RAM was used. Optimized implementation in a real-time operating system will speed up the computational efficiency even more.

Though the MFD and HCCI combustion models were separately validated, the validation of the integrated model is important because the temperature at the end of the combustion (the product of the HCCI combustion model) affects the thermodynamic state (pressure, temperature) of the next combustion event through the manifold filling dynamics (MFD model). The high dilution of this HCCI engine increases the significance of this internal feedback that generally exists to a smaller extent in conventional spark-ignition and compression-ignition internal combustion engines.

The orifice areas, C_dA_{01}, C_dA_{20}, and C_dA_{21} (u_{egr}) are calibrated using ambient condition $p_0=101$ kPa. The remaining inputs, u_{rbl}, and the fueling rate, W_f are the constant commanded values from the tests.

The steady-state flows are shown in Fig. 12. Due to the light throttle conditions, a deviation in p_1 causes a noticeable deviation in W_{01}. The maximum error appears in the case of 11 mg/cycle. Predictions of T_{ivc} show good accuracy, with the 11 mg point showing the greatest overprediction, as shown in Fig. 13.

Finally, consistent with reduced W_{01} for one of the 11 mg/cycle points shown in Fig. 12, the prediction of AFR at this operating point is lower, 19.5 vs 20 for the actual test data. This discrepancy in AFR prediction is shown in Fig. 14. Also, the higher value for T_{ivc} leads to a prediction of earlier θ_{soc} and performance variable θ_{CA50}. Note here that Figs. 12–14 show validation results for the fuel sweep and the sweep in the residual fraction (at fixed fuel at 11 mg/cycle) as indicated by the cluster of many stars at fuel equal to 11 mg/cycle.

Table 1 List of all parameters and their values, if constant

Parameter	Definition	Value (if constant)
α_1	Modulation of x_r by u_{bbl}	0.752
α_2	Modulation of x_r by u_{bbl}^2	−0.180
α_3	Modulation of x_r by u_{bbl}^3	0.015
β_0	Constant term of p_{ivc}	1.035 (KPa)
β_1	Linear term of p_{ivc}	1.1568
γ	Ratio of specific heats	
$\Delta\theta$	Burn duration	
ΔT_{bd}	Blowdown temperature difference	−65
κ_0	Constant term of x_r	−2.2107
κ_1	Linear term of x_r	61.5556
κ_2	p_2 exponent in x_r	4.6052
κ_3	p_1 exponent in x_r	0.964
θ_c	Angle of instantaneous heat release	
θ_{CA50}	Location of 50% fuel burned	
θ_{soc}	Location of start of combustion	
a_0	Constant term in e parametrization	1.0327
a_1	Linear term, e dependence on k	−5.45
A	Arrhenius scaling constant	2500
AFR	Air-to-fuel ratio (MAF/fuel rate)	
AFR_{EGO}	Air-to-fuel ratio, through exhaust sensor	
AFR_c	Air-to-fuel ratio in cylinder	
b_{k0}	const term in k parametrization	0.162
b_{k1}	Linear term in k dependence on θ_{soc}	0.005
b_{k2}	Square term in k dependence on θ_{soc}	0.001
e	Burn duration averaging parameter	
E_a	Arrhenius activation energy	6317
E_c	Activation energy	185 k J/mol
C_dA_{xy}	Orifice effective area between volume x to y	
b_{bd}	Burned gas fraction of blowdown gas	
b_{er}	Burned gas fraction in exhaust runner	
b_c	Burned gas fraction in cylinder at IVC	
b_x	Burned gas fraction of volume x	
k	Burn duration parameter	
m_x	Mass of gas in volume x	
m_{res}	Residual mass in cylinders	
m_c	Total mass in cylinder	
n	Polytropic constant	
n_{bd}	Adiabatic blowdown coefficient	1.35
n_c	Polytropic constant during compression	1.30
n_e	Polytropic constant during expansion	1.35
p_1	Mean Intake Manifold Pressure	
p_2	Mean Exhaust Manifold Pressure	
p_{bc}	Cylinder pressure before heat release	
p_{ac}	Cylinder pressure after heat release	
p_{ivc}	Cylinder pressure at intake valve closing	
R	gas constant, J/KgK	296.25
R_u	Universal gas constant, J/mol K	8.314
T_c	Temperature in cylinder	
T_{bc}	Cylinder temperature before heat release	
T_{ac}	Cylinder temperature after heat release	
T_{er}	Exhaust Runner Temperature	
T_{ivc}	Cylinder temperature at intake valve closing	
T_x	Temperature in volume x	
u_{egr}	EGR valve area, m^2	
u_{rbl}	Rebreathing valve lift mm	
W_{xy}	Mass flow rate from volume x to y	
W_c	Mean flow into cylinder (Kg/s)	
W_{egr}	EGR flow, same as W_{21} (Kg/s)	
W_f	Fuel flow rate (Kg/s)	
x_r	Residual gas fraction in cylinder	

9 Conclusions

We present a simple mean value model and validate it in steady state conditions. Specifically, the model has been validated at 1000 rpm, 7–12 mg/cycle, 20%–65% residual gas fraction (x_r), $\text{AFR}_{\text{ego}}=18-24$, intake and exhaust manifold pressure close to atmospheric pressure (unthrottled naturally aspirated conditions), and for gasoline fuel. Despite some discrepancies in the integrated model steady-state predictions, the trends in flows, states, conditions at IVC, and performance parameters are reproduced. Specifically, the model captures:

- the intake and exhaust manifold flows and the effects of the external and internal EGR
- the modulating effects of the actuators, u_{egr} and u_{rbl}
- the impact of the system state variables and actuators on the

performance variable, conventional AFR (inlet mass air flow rate/fuel flow rate), the tailpipe measured value, AFR_{EGO}, and the actual in-cylinder air-fuel ratio, AFR_c
- the impact of the system state variables and actuators on the performance variable θ_{soc} and θ_{CA50}

The model includes three continuous manifold states, three discrete cylinder states, and one sensor lag. Though the existing experimental setup did not allow the validation of transient behavior, the model can provide the basis for dynamical analysis and feedback control design of the HCCI engine.

Acknowledgments

We thank Sharon Liu, Jason Chen, and Man-Feng Chang of General Motors Corporation, George Lavoie of the University of Michigan, and Paul Ronney of the University of Southern California. Funding for this work was provided by the General Motors Corporation under Contract No. TCS-09026.

Appendix: Cylinder Mass and Temperature Calculations

In this appendix we provide the simple calculations for the cylinder mass trapped and cylinder temperature during steady-state conditions. We use parameters and variables introduced in Secs. 4–7, so the reader is advised to first study these sections and then read the calculations below.

The total mass trapped in the cylinder m_c is the summation of the mass coming from the intake manifold m_{im} and the residual mass trapped due to the rebreathing m_{res}.

$$m_c = m_{im} + m_{res} \tag{A1}$$

In steady state the mass from the intake manifold can be calculated based on the measured flows in the intake manifold

$$m_{im} = W_{1c}\tau = (W_{01} + W_{21})\tau \tag{A2}$$

The residual mass trapped at IVC can be approximated using the ideal gas law

$$m_{res} = \frac{p_{res}V_{ivc}}{RT_{er}} \tag{A3}$$

where p_{res} is the partial pressure of the residual mass trapped, V_{ivc} the cylinder volume at IVC, and the residual temperature is assumed to be equal to the exhaust runner temperature T_{er}. Dalton's law of partial pressures and another application of the ideal gas law provide the final measurable form for the residual mass estimation:

$$m_{res} = \frac{(p_{ivc} - p_{im})V_{ivc}}{RT_{er}} \tag{A4}$$

$$= \frac{p_{ivc}V_{ivc}}{RT_{er}} - \frac{m_{im}RT_1}{V_{ivc}}\frac{V_{ivc}}{RT_{er}} \tag{A5}$$

The steady-state total trapped mass can then be calculated as

$$m_c = \tau(W_{01} + W_{21})\left(1 - \frac{T_1}{T_{er}}\right) + \frac{p_{ivc}V_{ivc}}{RT_{er}}. \tag{A6}$$

The cylinder pressure measurements along with the estimated total mass trapped are then used for calculating the cylinder temperature when all the valves are closed.

References

[1] Najt P., and Foster, D., 1983, "Compression-Ignited Homogeneous Charge Combustion," SAE paper 830264

[2] Martinez-Frias, J., Aceves, S. M., Flowers, D., Smith, J. R., and Dibble, R., 2000, "HCCI Control by Thermal Management," SAE paper 2000-01-2869.

[3] Stanglmaier, D. S., and Roberts, E., 1999, "Homogenous Charge Compression Ignition (HCCI): Benefits, Compromises, and Future Engine Applications," SAE paper 1999-01-3682.

[4] Kontarakis, G., Collings, N., and Ma, T., 2000, "Demonstration of HCCI Using a Single Cylinder Four-stroke SI Engine With Modified Valve Timing," SAE paper 2000-01-2870.

[5] Shaver, G. M., Gerdes, J. C., Jain, P., Caton, P. A., and Edwards, C. F., 2003, "Modeling for Control of HCCI Engines," *Proc. of the American Control Conf.*, pp. 749–754.

[6] Shaver, G. M., and Gerdes, J. C., 2003, "Cycle-to-Cycle Control of HCCI Engines," *2003 ASME Proc. of International Mechanical Engineering Congress and Exposition*, IMECE2003-41966.

[7] Ohyama, Y., 2003, "Simultaneous Control of Air/fuel Ratio and Intake, Exhaust Valve Timing for HCCI Operation," SAE paper 2003-01-1084.

[8] Bengtsson, J., Strandh, P., Johansson, R., Tunestal, P., and Johansson, B., 2004, "Cycle-to-Cycle Control of a Dual-Fuel HCCI Engine," SAE paper 2004-01-0941.

[9] Olsson, J. O., Tunestal, P., and Johansson, B., 2001, "Closed Loop Control of an HCCI Engine," SAE paper 2001-01-1031.

[10] Agrell, F., Angstrom, H.-E., Eriksson B., and Linderyd, J., 2003, "Integrated Simulation and Engine Test of Closed Loop HCCI Control by Aid of Variable Valve Timing," SAE paper 2003-01-0748.

[11] Olsson, J. O., Tunestal, P., Johansson, B., Fiveland, S., Agama, R., Willi, M., and Assanis, D., 2002, "Compression Ratio Influence on Maximum Load of a Natural Gas Fueled HCCI Engine," SAE paper 2002-01-0111.

[12] Rausen, D. J., 2003, "A Dynamic Low Order Model of Homogeneous Charge Compression Ignition Engines," MS thesis, Mechanical Engineering, The University of Michigan.

[13] Heywood, J. B., 1988, *Internal Combustion Engine Fundamentals*, McGraw-Hill, Inc., New York.

[14] Grizzle, J., Buckland, J., and Sun, J., 2001, "Idle Speed Control of a Direct Injection Spark Ignition Stratified Charge Engine," Sitzungsber. Akad. Wiss. Wien, Math.-Naturwiss. Kl., Abt. 2A, **11**, pp. 1043–1071.

[15] Livengood, J. C., and Wu, P. C., 1955, "Correlation of Autoignition Phenomena in Internal Combustion Engines and Rapid Compression Machines," *5th Symposium on Combustion*.

[16] Willand, J., Nieberding, R.-G., Vent, G., and Enderle, C., 1998, "The Knocking Syndrome—Its Cure and Its Potential," SAE paper 982483.

[17] Ji, C., and Ronney, P. D., 2002, "Modeling of Engine Cyclic Variations by a Thermodynamic Model," SAE 2002-01-2736.

[18] Cantor, J. C., 1984, "A Dynamical Instability of Spark-Ignited Engines," Science, **224**, pp. 1233–1235.